J Therm Anal Calorim (2009) 98:441–448
DOI 10.1007/s10973-009-0322-y

Kinetics of the thermal decomposition of anhydrous cobalt nitrate by SCRT method

A. Ortega · M. Macías · F. J. Gotor

Received: 30 November 2008 / Accepted: 20 January 2009 / Published online: 12 August 2009

Abstract It has been shown the ability of the Sample Controlled Reaction Temperature (SCRT) method for both discriminate the kinetic law and calculate the activation energy of the reaction. This thermal decomposition is best described by a Johnson–Mehl–Avrami kinetic model (with $n = 2$) with an activation energy of nuclei growth which fall in the range 52–59 kJ mol^{-1}. The process is not a single-step because the initial rate of decomposition is likely to be limited by nucleation. The results reported here constitute the first attempt to use the new SCRT method to study the kinetic of the thermal decomposition of cobalt nitrate.

Keywords Cobalt Nitrate · Thermal analysis · Isoconversional methods · Reduced rate · Master plots · SCRT · Galwey method · Pseudoisotherm

Introduction

Cobalt nitrate is widely used as precursor for the preparation of the spinel p-type semiconductor Co_3O_4, which has found technological applications in many fields, such as heterogeneous catalysts [1], anode material in Li-ion rechargeable batteries [2], solid state sensors [2], solar energy absorbers [3], and electrode material for electrochemical capacitors [4]. The industrial importance of supported cobalt catalysts is well known, especially in Fisher–Tropsch (FT) synthesis [5] that maintains a current interest driven by the need of clean transportation fuels. On the other hand, the high catalytic activity of supported and unsupported cobalt oxide catalysts in CO and hydrocarbon oxidations makes this oxide a less expensive alternative to noble metal catalysts [1, 6]. The common method of preparation of Co-based supported catalysts involves the wet impregnation of the porous support material with a cobalt salt solution, generally $Co(NO_3)_2{\cdot}6H_2O$, and the subsequent thermal decomposition of the supported cobalt salt. Calcination is a critical step in the preparation of these catalysts. For example, significantly higher cobalt dispersion is found in catalysts prepared via low-temperature cobalt nitrate decomposition, leading to higher catalytic activity in FT synthesis [7].

A careful study of the decomposition mechanism of precursors of Co-based catalysts would help to clarify the relationship between the preparation method and the dispersion of supported metals. Also, particular emphasis should be placed in the use of thermal analysis methods in order to elucidate the factors affecting catalyst performance. To the best of our knowledge, few works concerning the thermal decomposition of cobalt nitrate have been done. In addition, these articles only focussed on the nature of the final product, the gases evolved during the decomposition or the formation of hydrated intermediate compounds [8–11]. It is rather surprising the lack of information concerning the kinetic mechanism of the thermal decomposition of this product. Only, Mu and Perlmutter [12] have performed the kinetic study from dynamic measurements (TG runs), but assuming an *n*th order kinetic model. However, it has been demonstrated [13] from non-isothermal experiments that all kinetic models fit appropriately the linear form of the kinetic equation, exhibiting the calculated activation energy value a strong dependence on the reaction model. Also, Lycourghiotis and Cotinopoulos [14] have studied the

A. Ortega (✉) · M. Macías · F. J. Gotor
Instituto de Ciencia de Materiales de Sevilla, Centro Mixto C.S.I.C/Universidad de Sevilla, Avda. Americo Vespucio s/n, 41092 Sevilla, Spain
e-mail: aortega@us.es

kinetics of decomposition of $Co(NO_3)_2$ from isothermal measurements, but on the surface of γ-Al_2O_3 or SiO_2, these authors indicate that among the various kinetic models tested (not shown in the article), a diffusion one (Jander equation) described well their experimental data.

The aim of this work is to study the mechanism of the thermal decomposition of cobalt nitrate in vacuum, and to calculate the activation energy of the reaction. This is part of a wider study of the influence of the experimental factors on the kinetics of solid state reactions. The literature data [15–17] have shown that experimental parameters such as sample mass and shape, particle size, ambient pressure, heating rate, etc. can affect significantly both the calculate value of the activation energy and the kinetic model controlling the reaction rate. The weak control of these parameters may be expected to be the cause of discrepancies [18–20]. The existence of these significant effects is a real limit to the kinetic understanding and to a consistent interpretation of solid state reactions. Therefore, a suitable method for controlling external parameters is needed; thus we defend the approach in which use is made of non conventional advanced techniques such as the Sample Controlled Reaction Temperature (SCRT). This method has been previously used to control the texture and structure of many materials [21–23], through kinetic control of the thermal reaction of their precursors, and it has been reported [24–26] that SCRT has higher sensitivity and resolution than conventional thermoanalytical methods (Isothermal and Non-isothermal).

Experimental

$Co(NO)_3{\cdot}6H_2O$ powder supplied by Merck with purity of >99% was used. The anhydrous salt was prepared by dehydrating the corresponding hexahydrate in situ at 378 K. This was the higher dehydration temperature could be used in order to avoid the decomposition of the nitrate salt. A Cahn electrobalance (model RG 2000) connected to a high vacuum system equipped with a penning gauge has been used for performing isothermal, non-isothermal and SCRT experiments. The pressure of the gases generated in the reaction was continuously monitored.

The temperature control in SCRT experiments is carried out in such a way that the decomposition rate is maintained constant throughout the process. This has been attained by interfacing the analogical output of the penning gauge to the furnace controller in order to maintain a constant residual pressure in the close vicinity of the sample. Thus, the reaction rate will be constant, provided that the pumping rate has been properly selected by means of a vacuum valve. Five curves have been carried out at $C = 0.00135, 0.00148, 0.00168, 0.0024$ and $0.0040\ min^{-1}$. Residual pressures ranging from 2×10^{-5} to 4×10^{-5} mbar have been selected. Sample weights ranging from 30 to 60 mg have been used in SCRT experiments. In order to elucidate the nature of gases produced during the thermal decomposition of cobalt nitrate and the stoichiometry of the global reaction, evolved gas analyses were performed by attaching the sample tube to a mass spectrometer fitted with a jet valve which eliminates mass lower than $m/e = 10$ (in order to avoid the He carrier gas). This system permits the recording of previously selected m/e peaks in order to determine the stoichiometry of the thermal decomposition of cobalt nitrate. The analysis of the nitric oxide, nitrogen dioxide, oxygen and water evolved during the reaction has been followed by monitoring simultaneously the mass peaks $m/e = 46$, 30, 32 and 18. Moreover, the $m/e = 30$ and $m/e = 46$ peak ratios are constant over the entire process at a value of $NO_2/NO = 0.27$ in agreement with the value obtained from the cracking of pure nitrogen dioxide in the vacuum chamber of the mass spectrometer. Therefore, it can be concluded that only nitrogen dioxide and oxygen are evolved during the thermal decomposition of anhydrous cobalt nitrate as previously reported [11] and consequently the above reaction take place according to the following overall equation:

$$3Co(NO_3)_2 \longrightarrow Co_3O_4 + 6NO_2 + O_2$$

The Co_3O_4 is the final product of decomposition, this agree with previous reports [27, 28]. On the other hand, analysis of evolved gases allows us to ascertain that the loss of water and the decomposition occurs in two independent steps, but in dynamic measurements this decomposition starts prior to total dehydration [6, 10]. The SCRT method allows us to separate completely the steps corresponding to the dehydration of the remainder crystallisation water and the nitrate decomposition because the principle of SCRT method is to control directly the reaction rate. Thus, we have check that the obtained experimental data only involve the nitrate thermal decomposition.

Kinetics equations

Advanced non-conventional methods (SCRT method)

If we use α to denote the extent of reaction, then the basic kinetic rate equation is usually taken as:

$$\frac{d\alpha}{dt} = K(T)f(\alpha) \quad (1)$$

where T is the temperature, $K(T)$ is the temperature-dependent rate constant given as:

$$K(T) = A\ \exp(-E/RT) \tag{2}$$

A and E are the pre-exponential factor and activation energy, respectively, and $f(\alpha)$ is the kinetic model function(see Table 1). In this paper, we use the Sample Controlled Reaction Temperature, SCRT (or CRTA) method. This method [29] is a temperature management technique where the temperature profile, required maintaining the partial pressure of evolved gases constant during the course of reaction, is recorded as a function of time. Because the partial pressure of the gases is proportional to the rate, the reaction proceeds at a constant overall decomposition rate, previously selected by the user, under a constant partial pressure of evolved gas. Comparison between SCRT approach and the conventional methods has been systematically carried out and is reported in numerous papers [30, 31]. Previous works have demonstrated the efficiency of SCRT to control the influence of experimental factor such as sample mass, particle size, heat and mass transfer effect [32–34]. SCRT permits both a good control of pressure in the close vicinity of the sample and the use of reaction rates low enough to keep temperature gradients at a negligible level to avoid any heat or mass transfer problems. If the process is carried out at a constant reaction rate C from Eqs. 1 and 2 we get:

$$C = A\ \exp(-E/RT)\, f(\alpha) \tag{3}$$

Equation 3 can be written as:

$$\ln \frac{1}{f(\alpha)} = \ln \frac{A}{C} - \frac{E}{R\,T} \tag{4}$$

Equation 4 shows that the higher the value C, the higher must be the temperature at which a particular value of α is reached. The plot of the left-hand side of Eq. 4 against the reciprocal of the temperature gives the values of the activation energy when the "Model-Fitting" method is used.

Master plots equations

Master plots are reference theoretical curves depending on the kinetic model but generally independent of the kinetic parameters of the reaction. By introducing the generalized time θ, Ozawa [35, 36] constructed the generalized kinetic equation at infinite temperature (θ = t when $T = \infty$). The generalized time defined as:

$$\theta = \int_0^t \exp(-E/RT)dt \tag{5}$$

where θ denotes the reaction time taken to attain a particular α at infinite temperature. Differentiation of Eq. 5 leads to

$$\frac{d\theta}{dt} = \exp(-E/RT) \tag{6}$$

From Eqs. 1 and 6, the following expression is obtained [37]:

$$\frac{d\alpha}{d\theta} = Af(\alpha) \tag{7}$$

which from Eq. 1 give rises to:

$$\frac{d\alpha}{d\theta} = \frac{d\alpha}{dt}\exp(E/RT) \tag{8}$$

where $d\alpha/d\theta$ correspond to the generalized reaction rate, obtained by extrapolating the reaction rate in real time, $d\alpha/dt$, to infinite temperature. The integrated form of the kinetic rate equation is obtained from Eq. 7 as follows:

$$g(\alpha) = \int_0^\alpha \frac{d\alpha}{f(\alpha)} = A\int_0^\theta d\theta = A\theta \tag{9}$$

From Eq. 7, the following equation is easily derived [38]:

$$\frac{d\alpha/d\theta}{(d\alpha/d\theta)_{0.9}} = \frac{f(\alpha)}{f(0.9)} \tag{10}$$

at a given α, in this paper, 0.9, the calculated value of the reduced-generalized reaction rate $d\alpha/d\theta/(d\alpha/d\theta)_{0.9}$ and the theoretical calculated value of $f(\alpha)/f(0.9)$ are equivalent when an appropriate $f(\alpha)$ is applied, then the experimental plot of $d\alpha/d\theta/(d\alpha/d\theta)_{0.9}$ against α is methodologically identical to the conventional master plots. According to Eq. 8, the reduced-generalized reaction rate has the following relationship to the experimental data:

Table 1 Set of reaction model to describe the reaction kinetics in solid-state reactions

Symbol	Model	Differential $f(\alpha)$ function	Integral $g(\alpha)$ function
JMA (A_n)	Nucleation and Growth (n = 0.5, 1, 1.5, 2, 2.5, 3, 4)	$n(1-\alpha)[-\ln(1-\alpha)]^{1-1/n}$	$[-\ln(1-\alpha)]^{1/n}$
R_n	Phase-Boundary Controlled reaction n = 0, 1/2 and 2/3	$(1-\alpha)^n$	$(1-(1-\alpha)^{1-n})/1-n$
D1	1D-Diffusion	$1/2\alpha$	α^2
D2	2D-Diffusion	$-1/\ln(1-\alpha)$	$\alpha + (1-\alpha)\ln(1-\alpha)$
D3	3D-Diffusion (Jander Equation)	$[3(1-\alpha)^{2/3}]/[2[1-(1-\alpha)^{1/3}]]$	$[1-(1-\alpha)^{1/3}]^2$
D4	3D-Diffusion (Ginstling–Brounshteinn Equation)	$3/2[(1-\alpha)^{-1/3}-1]$	$1-2\alpha/3-(1-\alpha)^{2/3}$

$$\frac{d\alpha/d\theta}{(d\alpha/d\theta)_{0.9}} = \frac{d\alpha/dt}{(d\alpha/dt)_{0.9}} \frac{\exp(E/RT)}{\exp(E/RT_{0.9})} \quad (11)$$

For calculating the experimental value of $(d\alpha/d\theta)/(d\alpha/d\theta)_{0.9}$ the temperature conditions have to be taken into account. Thus under isothermal condition, both the exponential term in Eq. 11 offset each other, so that the experimental master plot can be derived directly from a single isothermal curve of $d\alpha/dt$ against α. For the nonlinear non-isothermal data such as SCRT only the differential master plots can be calculated [38], the ratio of rate terms in Eq. 11 is to be unity. Thus, in this case, Eq. 11 reduces to:

$$\frac{d\alpha/d\theta}{(d\alpha/d\theta)_{\alpha=0.9}} = \frac{\exp(E/RT)}{\exp(E/RT_{0.9})} \quad (12)$$

Isoconversional method

The method proposed by Galwey [39] is more rigorous from a kinetic point of view than conventional isoconversional methods and is applicable to an arbitrary temperature program (Isothermal, TG, SCRTA, Stepwise Isothermal Analysis (SIA) or High Resolution Thermogravimetry (HRTG)) and permits to calculate the reaction model from a set of pseudoisothermal. This alternative proposal is based on the use of several non-isothermal experiments (under linear or nonlinear heating rate). Each data set is divided into stepwise small increments, $\Delta\alpha_i$ and Δt_i. The mean temperature T_i of each step is calculated. Thus, we assume an approximated linear rate of reaction within each small step (i.e., zero order reaction). The rate constant k_i at T_i is given by:

$$k_i = \frac{\Delta\alpha_i}{\Delta t_i} \quad (13)$$

Then from each set of k_i values the activation energy E_i can be calculated. Figure 1 shows a diagram of the method. A comparison of E_i values, corresponding to each sequential step that contributes to the completed reaction, identifies any variation with α. Finally the pseudoisothermal curves can be constructed [39]. In each SCRT curve, a representative T_R temperature is selected (the mean temperature of the SCRT interval of temperature for example) then, the rate constants, K_R, for each reaction interval $\Delta\alpha_i$, can be calculated for the temperature T_R using values of k_i and the calculated activation energy. Summation of the time intervals required to complete each successive reaction step then enables a set of $\alpha - t$ values that represent a pseudoisothermal reaction at T_R to be obtained. These pseudoisothermal are used later for elucidate the reaction model.

Results

Determination of the activation energy by the model fitting method

The SCRT curves obtained at different values of the reaction rates C are displayed in Fig. 2. Following the model fitting procedure, the plot of the left-hand side of Eq. 4 against the reciprocal of the temperature gives the values of the activation energy for SCRT data.

The sets of activation energies calculated by means of SCRT procedure (Eq. 4, model fitting method), for the thermal decomposition of cobalt nitrate, are shown in Table 2. In solid state decompositions, the induction period is usually associated with nucleation, i.e., the formation of reaction centers (nuclei). The SCRT curves with $C = 0.00135$, 0.00148, 0.00168 and 0.0024 show an induction period. In thermal decomposition processes, this is frequently followed by nuclei growth. Depending on the rates of nucleation and nuclei growth [40], the initial decomposition rate may be limited by either of the two

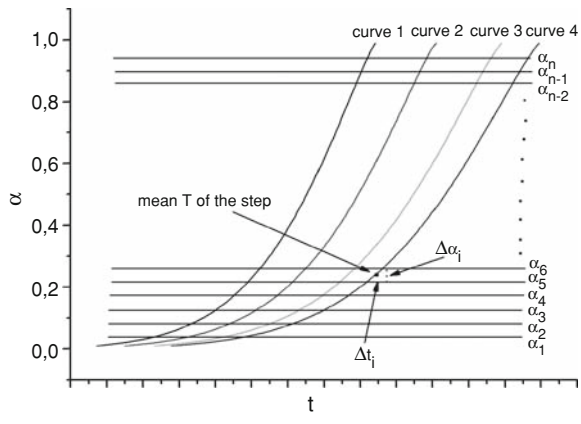

Fig. 1 Sketch of isoconversional approach based on zero order (Galwey method)

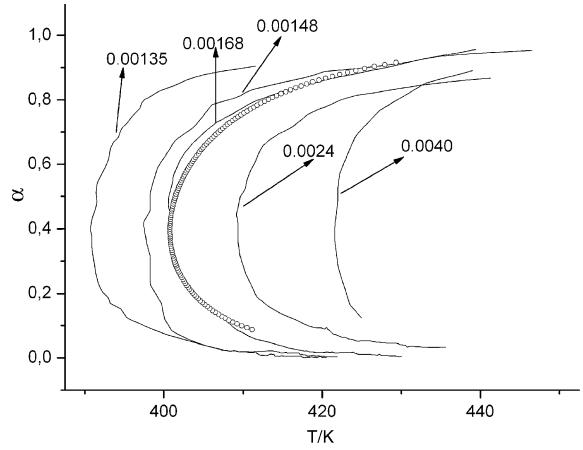

Fig. 2 SCRT curves of the thermal decomposition of Cobalt Nitrate at different constant reaction rates C

Table 2 Activation energies for thermal decomposition of cobalt nitrate at $C = 0.00168$ min^{-1} determined using model fitting method (Eq. 4) for SCRT data (range of α: 0.2–0.9) and other statistics

Model	E/kJ mol^{-1} Eq. 4	% s_b	s_{yx}	r	F-test Eq. 14
R1	Negative value	–	–	–	–
R2	42.3 ± 8.2	9.05	0.25	0.7440	16.91
R3	47.2 ± 10.1	9.10	0.33	0.7440	80.98
JMA ($n = 1$)	85.8 ± 7.1	9.10	0.50	0.7440	1192.31
JMA ($n = 2$)	58.5 ± 2.1	0.02	0.06	0.9990	1.00
JMA ($n = 3$)	49.9 ± 7.3	6.60	0.21	0.8350	26.27
D1	Negative value	–	–	–	–
D2	53.7 ± 33.1	30.40	1.05	0.3155	2879.46
D3	97.9 ± 34.3	20.70	1.30	0.4380	34177.72
D4	64.3 ± 36.2	25.51	1.14	0.3680	7109.49

processes. In the SCRT experiments, the slow temperature changes at the initial rate of decomposition favours the nucleation, thus we may expect that the constant decomposition rate gives rise to a constant rate of nucleation, thus the initial rate of decomposition is likely to be limited by nucleation in the SCRT experiments.

Thus, the activation energy calculated at $\alpha < 0.15$ from SCRT data ($E \approx 65$ kJ mol^{-1}) corresponds to the initial process of nucleation. The situation when the activation energy for nucleation is greater than that for growth is very frequent [40]. The appearance and growth of nuclei of the product (incipient phase) is a frequent and important stage in many processes of thermal decomposition: such as hydrates, oxalates, nitrates, carbonates etc. The initial reaction centers are formed together with subsequent development of stable nuclei of the product, and growth of the later to form a boundary between the old and the new phases. Since the middle 1920s, in solid-state kinetics, the concept of nucleation in thermal decomposition became more and more obvious. In their study of the thermal decomposition of silver oxalate, MacDonald and Hinshelwood [41] suggested for the first time that the decomposition involves two different rate processes, which are the formation of silver nuclei and their subsequent growth. These authors introduced the idea of the formation and growth of product nuclei in a decomposing solid. For the thermal decomposition of mercury fulminate, Garner and Hailes [42] suggested that nucleation is accompanied by the process of nuclei branching, which is characterized by its own rate constant. Jacobs and Tompkins [43] gave the first representative account of these mechanism and corresponding equations. In the classical text of Delmon [44] more details on nucleation and growth of nuclei can be found. The most recent compendium of these reaction models in thermal decomposition of solids is given by Galwey and Brown [45].

The resulting value of the model fitting method shown in Table 2 allows the Avrami–Erofeev model, JMA with $n = 2$, to be identified as the best description for the thermal decomposition of Cobalt Nitrate. The activation energy obtained, in the range of $\alpha = 0.2$–0.9, from model fitting procedure, is 58.5 kJ mol^{-1} and the pre-exponential factor, ln $A = 11.24$ min^{-1}. The model fitting procedure works well in this case but this routine ignores that the correlation coefficient is subject to random fluctuations and its uncertainty must be taken into account in the form of confidence limits. Thus, it is necessary to give a proper statistical treatment.

Determination of the kinetic model by SCRT master plots

To choose an appropriate reaction model the reduced master plots [38] are an interesting method. For each model, a useful measure of the "adequacy of fit" is the standard deviation of the residuals SS^2 with $n - 1$ degree of freedom. For each model, the adequacy of fit can be determined by using Eqs. 12 and 14.

$$SS^2 = \frac{1}{n-1}\sum_{i}^{n}\left(\frac{(d\alpha/d\theta)_i}{(d\alpha/d\theta)_{0.9}} - \frac{f(\alpha_i)}{f(0.9)}\right) \tag{14}$$

For random samples of size n_1 and n_2, and whose distributions are normal (where S_1^2 and S_2^2 are the standard deviations) the ratio S_1^2/S_2^2 (where the S_1 is the larger value) is distributed as Fisher's F with $n - 1$ degree of freedom [46–49]. If we wish to determine whether these could have come from normal populations having the same variance we check with an appropriate statistical test called the F-test. The Null Hypothesis H_0 (i.e., both variances are equal) is rejected if F is larger than the appropriate critical value, at the chosen level of significance, obtained from F Tables [47]. In our study we calculate $SS^2/SS^2_{\min}$, this statistic have also the F-distribution, thus for all the reaction models, the value $F^* = SS^2/SS^2_{\min}$ is then compared with the critical value $F_{\alpha,n-1,n-1}$. Those reaction models for which $F^* < F_{\alpha,n-1,n-1}$ with a significance level α (in this study $\alpha = 0.05$) belong to the set of adequacy fit. The value $F_{\alpha,n-1,n-1}$ is the appropriate critical value obtained from the F table, this value is a percentile of the F-distribution for a particular level of statistical probability, 100 $(1 - \alpha)$%, and correspond to the upper percentage point of the F-distribution.

For calculating the experimental master plots, the previously determined activation energy $E = 58.5$ kJ mol^{-1}, which correspond to the model that exhibit the best fit in Table 2, was assumed. For each model, the adequacy of fit can be determined by using the residual sum of squares, Eqs. 12 and 14 and the F-test for SCRT data.

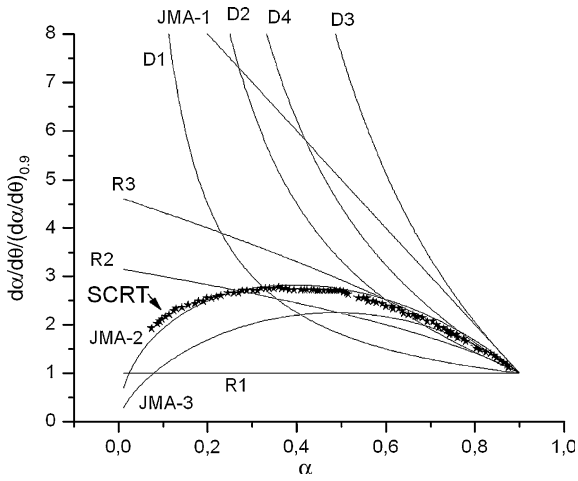

Fig. 3 Reduced reaction rate master plots for the thermal decomposition of cobalt nitrate for $\alpha = 0.9$ (Eq. 12) under SCRT. The JMA-2 gives the best fit

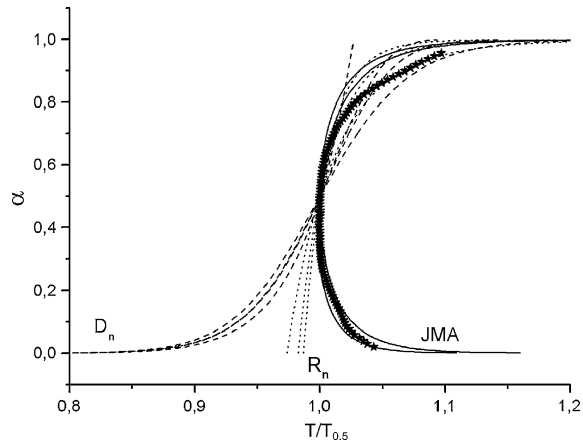

Fig. 4 Comparison between the shape of the theoretical SCRT for all the models in Table 1 and the experimental data for $C = 0.00168$ min^{-1} (*thick solid line*) in normalized temperature scale

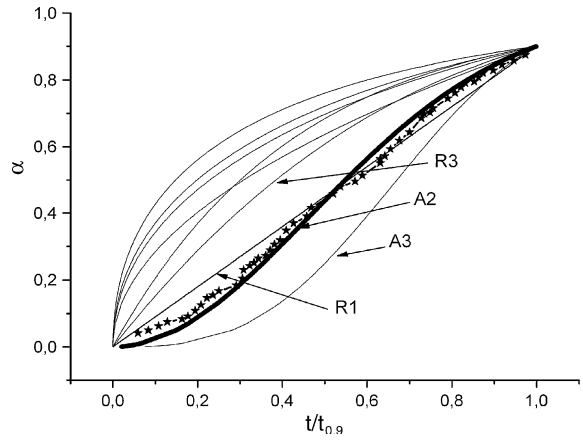

Fig. 5 Reduced time plots. Stars correspond to data that are the average of five pseudoisothermal experiments. The *solid line* correspond to the theoretical A2 kinetic model, the best fit

It is clearly seen from Fig. 3 and data of Table 2 that the experimental master plot corresponding to SCRT temperature profile are in excellent agreement with the theoretical master plot corresponding to JMA-2. All other reaction models should be discriminated as giving SS^2 values that are significantly larger than SS^2_{min} and F^* values greater than the critical F value and therefore rejected. The R1 and D1 kinetic models exhibit negative activation energy and the others Dn models very bad linear correlation coefficients ($r < 0.4$) and have been rejected. The other SCRT experiments, included in Fig. 2, analyzed at different constant reaction rate C show the same trend.

Another test for ascertain this result is the analysis of the shape of SCRT traces, because there is a correlation between the shape of SCRT curves and the kinetics [50], thus, this provide valuable information for elucidating the actual kinetic model obeyed by the reaction. A mere glance at the shape of the SCRT curves provides an easy way of discriminating between the different mechanisms of Table 1. Figure 4 shows the set of isokinetic theoretical SCRT curves and, in particular, we can see that the shape of JMA (*An*) kinetic models are very characteristic. Figure 4 shows that the experimental SCRT curve of the thermal decomposition of cobalt nitrate is similar in shape to the JMA kinetic models (*An*), this shape is characteristic of an Avrami–Erofeev model with a minimum on the T axis

To confirm this result and to extract the maximum information from the experimental data, a set of $\alpha - t$ pseudoisothermal data have been obtained from the SCRT experimental curves, following the Galwey methods [39]. The set of T_R temperatures (the mean temperature of the SCRT interval) are obtained. One can plot α as a function of a reduced time variable $t/t_{0.9}$ where $t_{0.9}$ is the time required to reach a 90% of conversion in each pseudoisotherm, this reduced time method is broadly used in solid state kinetics [51]. The reduced time plots for the thermal decomposition of cobalt nitrate is shown in Fig. 5 and this confirm the JMA-2 kinetic model.

Test for the dependence of the activation energy on the extent of conversion

The application of the isoconversional method permits a determination of the activation energy as a function of the degree of conversion α. Unlike the model fitting method, which yields a single overall value of activation energy for the process (58.5 kJ mol^{-1}) the isoconversional technique may reveal complexity of the reaction mechanism in the form of a functional dependence of the activation energy on the extent of conversion. Because most solid-state reactions are not simple one-step processes, analysis of

Table 3 Activation energies calculated with the isoconversional method based on zero order, from SCRT curves

Interval	E value/kJ mol^{-1}	r
0.2–0.3	56.5	0.9989
0.3–0.4	55.3	0.9987
0.4–0.5	54.8	0.9988
0.5–0.6	54.4	0.9985
0.6–0.7	55.3	0.9988
0.7–0.8	57.3	0.9987

Mean value SCRT = 55.6 KJ mol^{-1}. In each interval 50 measures have been taken

Table 4 Physical meaning of the JMA kinetic coefficient

Type of nucleation and geometry of growing	Law of growing of nuclei	
	Chemical reaction (linear law) n	Diffusion (parabolic law) n
Instantaneous nucleation and one-dimensional growth	1.0	0.5
Instantaneous nucleation and two-dimensional growth	2.0	1.0
Instantaneous nucleation and three-dimensional growth	3.0	1.5
Constant rate of nucleation and one-dimensional growth	2.0	1.5
Constant rate of nucleation and two-dimensional growth	3.0	2.0
Constant rate of nucleation and three-dimensional growth	4.0	2.5

SCRT data by the isoconversional technique is a good procedure to revealing this type of complexity.

Table 3 shows the values of the activation energies obtained from the set of SCRT curves with the use of this isoconversional approach based in zero order (Galwey method Eq. 13).

We can see in Table 3 that a systematic changes of E with α is not observed, the value obtained from SCRT isoconversional method, 55.6 kJ mol^{-1} is consistent with the value obtained in Table 2 for the JMA-2 kinetic model, 58.5 kJ mol^{-1}, and this kinetic model shows the best fit in Figs. 3 and 5, thus statistical analysis allows this model to be chosen with the exclusion of all others in Table 1, but again, we must take into account that perhaps the correct model is not included in this Table, this uncertainty is always present.

Conclusions

When SCRT data are analyzed there are consistent results among the three experimental procedure: model fitting, isoconversional and pseudoisothermal and the statistical analysis (F-test) allows the Avrami–Erofeev (JMA with $n = 2$) model to be identified as the best description for the thermal decomposition of anhydrous cobalt nitrate, the activation energy obtained fall in the range 54–59 kJ mol^{-1}, but the initial stage of decomposition give rise to an activation energy of 65 kJ mol^{-1} which correspond to the nucleation process. According to the original theory [52], n should be an integer from 0.5 to 4, the value of which should depend only on the type of the statistical model. The JMA theory describes the kinetics of phase transformation using the Eq. $1 - \alpha = 1 - \exp(-kt^n)$ where k and n depend on geometric factors and on the mechanisms of formation of nuclei and the number of spatial dimensions in which the crystal grows, as summarised in Table 4.

This table shows that a same n-parameter would describe different reaction mechanisms. The results here obtained would be interpreted by considering that the reaction mechanism implies the constant rate of nucleation in the bulk and their subsequent two-dimensional growth through a diffusion process. Such a mechanism leads to the fitting of the kinetic data to an Avrami coefficient $n = 2$.

References

1. El-Shobaby GA, Deraz NAM. Surface and catalytic properties of cobaltic oxide supported on an active magnesia. Mater Lett. 2001;47:231–40.
2. Li WY, Xu LN, Chen J. Co_3O_4 nanomaterials in lithium-ion batteries and gas sensors. Adv Funct Mater. 2005;15:851–7.
3. Avila A, Barrera E, Huerta L, Muhl S. Cobalt oxide films for solar selective surfaces, obtained by spray pyrolysis. Sol Energy Mater Sol Cells. 2004;82:269–78.
4. Cao L, Lu M, Li HL. Preparation of mesoporous nanocrystalline Co_3O_4 and its applicability of porosity to the formation of electrochemical capacitance. J Electrochem Soc. 2005;152:A871–5.
5. Schulz H. Short history and present trends of Fischer–Tropsch synthesis. Appl Catal A. 1999;186:3–12.
6. Tiernan MJ, Fesenko EA, Barnes PA, Parkes GMB, Ronane M. The application of CRTA and linear heating thermoanalytical techniques to the study of supported cobalt oxide methane combustion catalysts. Thermochim Acta. 2001;379:163–72.
7. Girardon JS, Lermontov AS, Gengembre L, Chernavskii PA, Griboval-Constant A, Khodakov AY. Effect of cobalt precursor and pretreatment conditions on the structure and catalytic performance of cobalt silica-supported Fischer–Tropsch catalysts. J Catal. 2005;230:339–52.
8. Simmons EL, Wendlandt WW. The thermal deaquation of some cobalt(II) salt hydrates. Thermochim Acta. 1971;3:25–36.
9. Mehandjiev D, Nikolova-Zhecheva E. Mechanism of the decomposition of cobaltous compounds in vacuo. Thermochim Acta. 1980;37:145–54.
10. Mansour SAA. Spectrothermal studies on the decomposition course of cobalt oxysalts Part II. Cobalt nitrate hexahydrate. Mater Chem Phys. 1996;36:317–23.
11. Cseri T, Bekassy S, Kenessey G, Liptay G, Figueras F. Characterization of metal nitrates and clay supported metal nitrates by thermal analysis. Thermochim Acta. 1996;288:137–54.

12. Mu J, Perlmutter DD. Thermal decomposition of metal nitrates and their hydrates. Thermochim Acta. 1982;56:253–60.
13. Criado JM, Ortega A. Errors in the determination of activation energies of solid-state reactions by the Piloyan method, as a function of the reaction mechanism. J Therm Anal. 1984;29: 1075–82.
14. Lycourghiotis A, Cotinopoulos M. Kinetics of the decomposition of cobalt nitrate on the surface of gamma-Al_2O_3 and SiO_2. React Solids. 1985;1:95–9.
15. Gallagher PK, Johson DW Jr. The effects of sample size and heating rate on the kinetics of the thermal decomposition of $CaCO_3$. Thermochim Acta. 1973;6:67–83.
16. Lahiri AK. The effect of particle size distribution on TG. Thermochim Acta. 1980;40:289–95.
17. Simon JJ. Some considerations regarding the kinetics of solid-state reactions. J Therm Anal. 1973;5:271–84.
18. Sestak J. Errors of kinetic data obtained from thermogravimetric curves at increasing temperature. Talanta. 1966;13:567–79.
19. Flynn JH. The effect of heating rate upon the coupling of complex reactions. I. Independent and competitive reactions. Thermochim Acta. 1980;37:225–38.
20. Criado JM, Rouquerol F, Rouquerol J. Thermal decomposition reactions in solids: comparison of the constant decomposition rate thermal analysis with the conventional TG method. Thermochim Acta. 1980;38:109–15.
21. Alcala MD, Criado JM, Real C. Sample controlled reaction temperature (SCRT): controlling the phase composition of silicon nitride obtained by carbothermal reduction. Adv Eng Mater. 2002;4(7):478–82.
22. Criado JM, Gotor FJ, Ortega A, Real C. The new method of constant rate thermal analysis (CRTA): application to discrimination of the kinetic model of solid state reactions and the synthesis of materials. Thermochim Acta. 1992;199:235–8.
23. Criado JM. Application of SCTA methods for kinetic analysis of solid state reactions and synthesis of materials. J Therm Anal Calorim. 2003;72:1097–8.
24. Ortega A. The kinetics of solid-state reactions toward consensus—Part I. Uncertainties, failures, and successes of conventional methods. Int J Chem Kinet. 2001;33:343–53.
25. Ortega A. The kinetics of solid-state reactions toward consensus, Part 2: fitting kinetics data in dynamic conventional thermal analysis. Int J Chem Kinet. 2002;34:193–208.
26. Ortega A. The kinetics of solid-state reactions toward consensus, Part 3. Searching for consistent kinetic results: SCTA vs. conventional thermal analysis. Int J Chem Kinet. 2002;34:223–36.
27. Ehrhard C, Gjikaj M, Brockner W. Thermal decomposition of cobalt nitrato compounds: Preparation of anhydrous cobalt(II)-nitrate and its characterisation by Infrared and Raman spectra. Thermochim Acta. 2005;432:36–40.
28. Brockner W, Ehrhard C, Gjikaj M. Thermal decomposition of nickel nitrate hexahydrate, $Ni(NO_3)_2{\cdot}6H_2O$, in comparison to $Co(NO_3)_2{\cdot}6H_2O$ and $Ca(NO_3)_2{\cdot}4H_2O$. Thermochim Acta. 2007;456:64–8.
29. Rouquerol J. L'analyse thermique a vitesse de decomposition constante. J Therm Anal. 1970;2:123–40.
30. Ortega A. CRTA or TG? Thermochim Acta. 1997;298:205–14.
31. Ortega A, Akhouayri S, Rouquerol F, Rouquerol J. On the suitability of controlled transformation rate thermal analysis (CRTA) for kinetic studies, Part 2. Comparison with conventional TG for the thermolysis of dolomite with different particle sizes. Thermochim Acta. 1994;235:197–2004.
32. Ortega A, Perez-Maqueda LA, Criado JM. The problem of discerning Avrami-Erofeev kinetic models from the new controlled rate thermal analysis with constant acceleration of the transformation. Thermochim Acta. 1995;254:147–52.
33. Ortega A, Akhouayri S, Rouquerol F, Rouquerol J. On the suitability of controlled transformation rate thermal analysis (CRTA) for kinetic studies. 3. Discrimination of the reaction mechanism of dolomite thermolysis. Thermochim Acta. 1994;247:321.
34. Criado JM, Ortega A, Rouquerol J, Rouquerol F. Influence of pressure on the shape of TG and controlled transformation rate thermal analysis (CRTA) traces. Thermochim Acta. 1994;240: 247–53.
35. Ozawa T. A new method of analyzing thermogravimetric data. Bull Chem Soc Jpn. 1965;38:1881–6.
36. Ozawa T. Non-isothermal kinetics and generalized time. Thermochim Acta. 1986;100:109–18.
37. Ozawa T. Applicability of Friedman plot. J Thermal Anal. 1986;31:547–51.
38. Gotor FJ, Criado JM, Malek J, Koga N. Kinetic analysis of solid-state reactions: the universality of master plots for analyzing isothermal and nonisothermal experiments. J Phys Chem A. 2007;104(46):10777–82.
39. Galwey AK. Perennial problems and promising prospects in the kinetic analysis of nonisothermal rate data. Thermochim Acta. 2003;407:93–103.
40. Vyazovkin S, Wight CA. Kinetics of thermal decomposition of cubic ammonium perchlorate. Chem Mater. 1999;11:3386–93.
41. MacDonald JY, Hinshelwood CN. The formation and growth of silver nuclei in the decomposition of silver oxalate. J Chem Soc. 1925;127:2764–71.
42. Garner WE, Hailes HR. Thermal decomposition and detonation of mercury fulminate. Proc R Soc Lond A. 1933;139:576–95.
43. Jacobs PWM, Tompkins FC. Chemistry of the solid state. In: Garner WE, editor. Chemistry of the solid state, Chap. 8. London: Butterworth; 1955.
44. Delmon B. Introduction a la cinetique heterogene. Paris: Editions Technip; 1969.
45. Galwey AK, Brown ME. Thermal decomposition of ionic solids. Amsterdam: Elsevier; 1999.
46. Vyazovkin S, Wight CA. Model-free and model-fitting approaches to kinetic analysis of isothermal and nonisothermal data. Thermochim Acta. 1999;340–341:53–68.
47. Zar JH. Biostatistical analysis. 4th ed. Englewood Cliffs, NJ: Prentice-Hall Inc.; 1998.
48. Green JR. Testing the agreement of data with a kinetic mechanism. Trans Faraday Soc. 1969;65:3288–94.
49. Rodante F, et al. Kinetic analysis of single or multi-step decomposition processes: limits introduced by statistical analysis. J Therm Anal Calorim. 2002;68:689–713.
50. Criado JM, Ortega A, Gotor F. Correlation between the shape of controlled-rate thermal analysis curves and the kinetics of solid-state reactions. Thermochim Acta. 1990;157:171–9.
51. Brown ME, Dollimore D, Galwey AK. Reactions in the solid state. Comprehensive chemical kinetics, vol. 2. Amsterdam: Elsevier; 1980.
52. Avrami M. Kinetics of phase change. I General theory. J Phys Chem. 1939;7:1103–12.